Journal of Materials Chemistry B

RSC Publishing

PAPER

View Article Online
View Journal | View Issue

Cite this: J. Mater. Chem. B, 2013, 1, 801

Hemocompatible and antibiofouling PU-F127 nanospheres platform for application to glucose detection in whole blood

Chong Sun,†[ab] Libin Chen,†[a] Fujian Xu,[c] Peiyuan Zhu,[d] Jianfeng Luan,[d] Chun Mao*[a] and Jian Shen*[a]

Analysts are always enthusiastic about finding new materials with good biocompatibility to improve the behavior of biosensors. In this case, a novel electrochemical biosensor, which can be conveniently applied to veraciously evaluate the level of blood glucose with the help of antibiofouling technology, was prepared and investigated. More details of the preparation of polyurethane-Pluronic F127 (PU-F127) nanospheres and immobilizing glucose oxidase (GOx) on (PU-F127)–glass carbon electrode (GCE) were presented. The electrochemical behavior of the biosensor in whole blood was studied. The cyclic voltammetric results indicated that GOx immobilized on the PU-F127 nanospheres exhibited direct electron transfer reaction, which led to stable amperometric biosensing for glucose with a detection limit of 1.14×10^{-5} M ($S/N = 3$) in whole blood. The PU-F127 nanospheres modified GCE also offered good anti-interference ability to ascorbic acid (AA) and uric acid (UA), especially when a detection potential of −0.49 V was employed. The good stability and repeatability of this biosensor were also proved. The integration of the technologies, which include anticoagulants, sensors and nanoscience, will have significant input to high-performance biosensors relevant to diagnostics and therapies of interest for human health.

Received 10th October 2012
Accepted 23rd November 2012

DOI: 10.1039/c2tb00396a

www.rsc.org/MaterialsB

Introduction

Anti-biofouling surfaces lie at the heart of several contemporary and advanced technologies, ranging from coatings for biomedical implants, ship hulls, and carriers for targeted drug delivery.[1–8] In the past years, different approaches were taken by various research groups to combat the challenge of forming anti-biofouling and fouling release surfaces. Particular attention was given to the chemical structures produced and the various techniques utilized to demonstrate these surfaces' inherent anti-biofouling character.

In Reichert's review paper, he suggested that biofouling is one of several causes of the failure of *in vivo* biosensors due to the accumulation of proteins, cells and other biological materials on the surface of biosensors.[5] At present, it is very difficult to design and prepare an electrochemical biosensor that can be used in whole blood, because biofouling of the electrode surface can develop from platelet, fibrin and blood cell adhesion in the complex environment of whole blood media. As we know, when in direct contact with blood, foreign materials are prone to initiate the formation of clots, as platelets and other components of the blood coagulation system are activated. As for a glucose biosensor that is used in whole blood directly, the biofouling of the electrode surface will bring about catastrophic damage to the electron transfer between the enzyme and electrode redox center. Anti-biofouling is the process of removing or preventing these accumulations, including platelets and other components of the blood, from forming. So, improving the hemocompatibility and anti-biofouling properties of biomaterials or biodevices has become a very important task for biomedical materials scientists.

Until now, the primary methods of detecting blood glucose concentration are performed by biochemical analyzers and glucose meters.[9–11] In hospital, the quantification of the concentration of glucose is mainly carried out in serum samples by biochemical analyzers, which are isolated from whole blood by centrifugation, but not in untreated whole blood. The test results are influenced by the different model numbers of test instruments and detection reagents, the treatment processes of blood samples, especially additional centrifuging and too long

[a]Jiangsu Key Laboratory of Biofunctional Materials, College of Chemistry and Materials Science, Nanjing Normal University, Nanjing, 210023, China. E-mail: maochun127@yahoo.com.cn; shenjian@njnu.edu.cn

[b]School of Chemical Engineering, Nanjing University of Science and Technology, Nanjing, 210094, China

[c]Key Laboratory of Carbon Fiber and Functional Polymers, Ministry of Education, College of Materials Science and Engineering, Beijing University of Chemical Technology, Beijing, 100029, China

[d]Department of Blood Transfusion, Nanjing Jinling Hospital, Nanjing University School of Medicine, Nanjing, 210002, China

† Both authors contributed equally to this work.

measuring time from collecting a specimen of blood to examination. As for commercial glucose meters, accurate results for glucose concentration cannot be provided by a commercial glucose meter, due to the fact that some defects cannot be ignored during its operation. For example, blood samples are obtained from the fingertip peripheral but not veins, and doped easily with tissue fluid. So the development of novel glucose biosensors for antifouling, rapid, highly sensitive, and selective detection is of paramount importance for blood glucose concentration monitoring in whole blood samples.

Pluronic F127 (triblock copolymer $PEO_{106}PPO_{70}PEO_{106}$) has good blood compatibility.[12,13] In addition, it also can be used as a template for preparation of nanoparticles with specific shapes.[14,15] Many previous studies show that novel nanomaterials for use in bioassay applications represent a rapidly advancing field. Nanoparticles have dimensions similar to those of biomolecules such as enzymes. Therefore, the combination of biomolecules with nanostructures produces functional nanostructured bio-interfaces with synergistic functions and properties.[16] For example, nanostructured metal oxides (NMOs) have recently become important as materials that provide an effective surface for biomolecule immobilization with desired orientation, better conformation and high biological activity, resulting in enhanced sensing characteristics. Malhotra's group discussed the various approaches that had been adopted for improving the performance of NMOs-based biosensors for clinical and non-clinical applications.[17–19]

Recently, nanomaterials of polymers are found to have superior performance compared with conventional polymeric materials due to their much larger exposed surface area and better biocompatibility. Polyurethane (PU) nanoparticles, as a special class of colloidal dispersions, can be utilized in biological fluids, pharmaceuticals, coatings, foods, and cosmetics. The preparation of PU nanoparticles with specific functional groups, ions, or biomolecules requires the synthesis of polymers possessing such functionality through complex synthetic routes or post-functionalization of the PU nanoparticles with the moiety of interest. The preparation and blood compatibility of phosphorylated PU nanoparticles were investigated in our previous work.[20]

Here, a novel kind of polyurethane-Pluronic F127 (PU-F127) nanosphere was prepared and chosen to modify the GCE for its antibiofouling effect which is due to the coherence between the blood compatibility and antifouling properties of F127. Using hemocompatible polymeric nanospheres to do the study of antibiofouling of the glucose biosensor was attempted by our research group in this case.

Experimental section

Reagents

Medical grade PU was from Suzhou Kesong Polymer Co. Ltd. (China). Pluronic F127 and glucose oxidase (GOx) were purchased from Sigma-Aldrich Co. (USA); β-D-(+)-glucose (99%) was obtained from J&K Chemical Co. Inc. (China). Dimethylsulfoxide (DMSO) was purchased from Sinopharm Chemical Reagent Co. Ltd. and used as received. Phosphate buffer solution (PBS) was prepared by mixing stock standard solution of Na_2HPO_4 and NaH_2PO_4. All solutions were made up with twice-distilled water. Other reagents were of analytical grade.

Synthesis of PU-F127 nanospheres

The PU-F127 nanospheres were prepared by a spontaneous emulsion solvent diffusion method, as follows.[21] Typically, 40 mg of PU was dissolved in 2 mL DMSO at room temperature, then slowly added to 30 mL of twice-distilled water containing 1.5 g of Pluronic F127 with vigorous stirring. The resulting nanoparticle suspension had a blue tint (Tyndall effect). Then the suspension was purified by dialysis through a dialysis bag (MWCO 25 000) to remove organic components and excess F127. The same mixing process without F127 was repeated, and the PU particle sample acted as the control.

Characterization of PU-F127 nanospheres

Transmission electron microscopy (TEM) of the nanoparticles was performed with a HITACHI H-7650 interface high-resolution transmission electron microscope (HITACHI, Japan). The FTIR spectra of the PU-F127 nanospheres were measured using a VARIAN Cary 5000 Fourier transform infrared spectrophotometer (VARIAN, USA).

Coagulation tests of PU-F127 nanospheres

Whole blood from a healthy rabbit was collected and centrifuged at 300*g* for 20 min at 4 °C to separate the blood corpuscles, and the resulting platelet-rich plasma (PRP) was centrifuged at 2000*g* for 20 min at 4 °C to obtain the platelet-poor plasma (PPP) for adsorption of rabbit plasma protein tests. The nanoparticles were incubated in 0.5 mL of PPP at 37 °C for 1 h.[22] The activated partial thromboplastin time (APTT), prothrombin time (PT) and thrombin time (TT) of the PPP were then determined by using a semi-automated coagulometer (Rayto RT-2204C, USA). All the coagulation tests were performed in triplicate.

Complement activation and platelet activation

Hemocompatibility of the PU-F127 nanospheres was evaluated by measuring complement activation and platelet activation under *in vitro* conditions.[23,24] To assess the complement activation, the cleavage of the complement component C3 was monitored by measuring the formation of its activation peptides, C3a and C3a des-Arg, using a commercial C3a enzyme immunoassay kit with a flow cytometer (BD Biosciences FACSCalibur, USA) according to the manufacturer's instructions. The PPP of human blood and the PU-F127 nanospheres in saline were incubated at 37 °C for 1 h. All the complement activation experiments were done in triplicate.

To measure the platelet activation, the PRP of human blood was incubated at 37 °C with an equal volume of the PU-F127 nanospheres suspension in saline. The incubation mixture was removed at 30 min to assess the activation state of the platelets using fluorescence flow cytometry. Expression of the

fluorescently labeled platelet activation marker anti-CD62P and the platelet pan-marker anti-CD42a was detected using a BD FACSCalibur and a double staining method, according to the manufacturer's instructions. All the platelet activation experiments were done in triplicate.

Whole blood adhesion tests

The surface sections of blank GCE and GOx–(PU-F127) modified GCE were placed in individual wells of a 24-well tissue culture plate and each well was equilibrated with 1.0 mL of PBS for 24 h at 25 °C. To each well was added 1.0 mL of whole blood. After being incubated for 60 min at 37 °C in humidified air, the samples were taken out. After the GCEs were rinsed three times with PBS, they were immersed into 2.5% glutaraldehyde of PBS for 30 min to fix the adhered blood cells, then rinsed three times with PBS and gradient-dried with ethanol–water solutions (50, 60, 70, 80, 90, 95 and 100% (v/v)) for 30 min each and dried in air.[20,25–28] Finally, the samples were sputter-coated with gold prior to observation under a JEOL JSM-6300 scanning electron microscope (SEM).

Characterization of GOx–(PU-F127) bioconjugates

The circular dichroism (CD) spectra were taken by using a Jasco J-715 spectropolarimeter (Applied Photophysics, Great Britain). Quartz cells of 1 cm optical path length were used for all CD measurements of GOx (GOx concentration = 0.06 mg mL^{-1}) and GOx–PU-F127 (GOx : (PU-F127) = 1 : 1 weight ratio) solutions. The contents of α-helix, β-sheet, β-turn and the random coil conformation were calculated using the JASCO710 program.

Construction of GOx–(PU-F127)–GCE and glucose measurements

Prior to modification, the GCE was successively polished to a mirror-like surface with 0.3 and 0.05 μm alumina slurry followed by rinsing thoroughly with double-distilled water. After sonication in ethanol and double-distilled water for 5 min, respectively, the GCE was allowed to dry at room temperature. Then, 8.0 μL of the resulting PU-F127 nanospheres suspension was dropped onto the electrode surface and dried in air. After that, 8.0 μL of 6 mg mL^{-1} GOx solution was dropped onto the surface of (PU-F127)–GCE and kept overnight at 4 °C, then the GCE modified by GOx–(PU-F127) was obtained and the same modified method was used to get the GOx–F127–GCE and (PU-F127)–GCE. When not in use, the electrodes were stored at 4 °C in a refrigerator.

Cyclic voltammetry studies used a CHI 760D electrochemical workstation (Shanghai Chenhua, China). All experiments were carried out using a three-electrode cell equipped with a platinum electrode as counter electrode and saturated calomel electrode (SCE) as reference electrode. The working electrode was a GCE. The applied scan rate was 100 mV s^{-1}. Amperometric measurements were carried out using a three electrode cell consisting of an working electrode, a counter electrode of a platinum electrode, and a reference electrode of SCE. Cyclic voltammogram (CV) measurements were conducted in 5 mL of 0.1 M PBS, and the solution was purged with high purity nitrogen prior to and blanked with nitrogen during the electrochemical experiments. Amperometric detections were performed under an applied potential of −0.49 V. The responses were taken as the change between the steady state and background currents. Differential pulse voltammetry (DPV) measurements were carried out with a pulse amplitude of 0.05 V and a pulse width of 0.2 s. Different concentrations of glucose solution were added under intense stirring, then CV was performed until the currents did not change any more, and DPV was immediately carried out. Finally, the correlation between the response currents and different concentrations of glucose solution was obtained. Besides, the anti-interference properties of the biosensor were investigated by adding 0.1 mM glucose, followed by 10 mM AA, 0.1 mM glucose and 10 mM UA.

Results and discussion

Characterization of PU-F127 nanospheres

PU dispersions can be prepared from a mixture of different chemical species, in which the interfacial energy is very important. Here, the PU-F127 nanospheres were prepared by a spontaneous emulsion solvent diffusion method. As displayed in Fig. 1a, a typical TEM photograph of the PU-F127 nanospheres showed the average diameter is about 250 nm. It is very interesting that every PU-F127 nanosphere has a porous structure (Fig. 1b). This is a new shape that has not been reported previously. As to the control sample, Fig. 1c showed the TEM image of the PU particles. It could be observed that the PU particles were agglomerated severely in the absence of F127. The formation mechanism of this porous structure of PU-127 was not clear. It was speculated that this porous structure of the PU-127 nanospheres may be attributed to F127 that acts as a dispersant, dopant and porogen.[14,15,29] More investigation will be done by our research group in the near future.

Fig. 2 showed the FTIR absorption spectra in the 500–3800 cm^{-1} range of Pluronic F127, blank PU material, and the PU-F127 nanospheres. Fig. 2a showed the FTIR spectrum of Pluronic F127, from which one broad intense band around 1112 cm^{-1} with a shoulder around 1147 cm^{-1} could be seen, while the peak at 1063 cm^{-1} is distinctive of the helical structure of PEO (Fig. 2a).[30]

As shown in Fig. 2b, there were two obvious absorption peaks at 1728 and 1517 cm^{-1}, which are characteristic of the carbonyl vibration and the C–N vibration of PU.[31,32] After being trapped with F127, the presence of a band around 1728 cm^{-1} and a 1664 cm^{-1} band clearly showed that F127 had been trapped into PU nanoparticles (Fig. 2c). The two obvious absorption peaks at about 3500 and 2850 cm^{-1} were observed in the three FTIR absorption spectra of Fig. 2. The band at about 3500 cm^{-1} is characteristic of the OH stretching bands,[33] and the band at about 2850 cm^{-1} is attributed to the stretching vibration bands of $-CH_3$ and $-CH_2-$ in molecules.[34]

In vitro anticoagulation properties

The APTT, PT and TT were widely used for the clinical detection of the abnormality of blood plasma. In recent times, they were

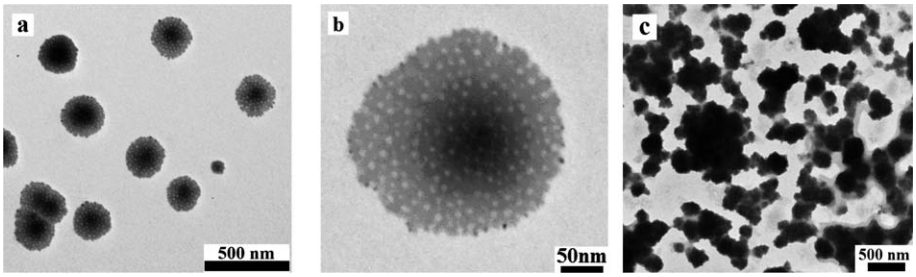

Fig. 1 Representative TEM images of (a) PU-F127 nanospheres, (b) enlarged TEM image of a single PU-F127 nanosphere, and (c) PU particles without F127.

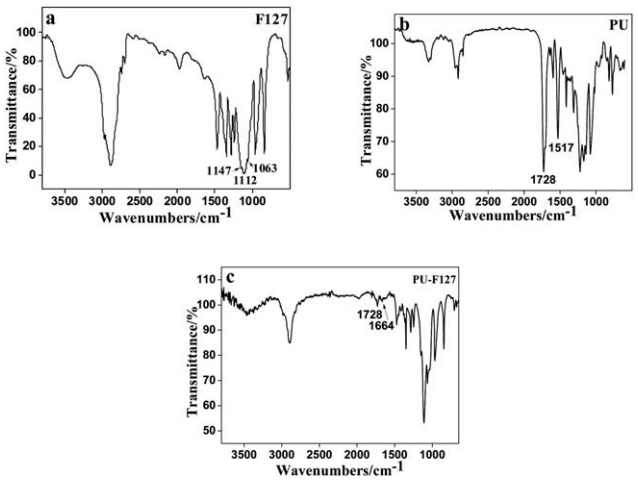

Fig. 2 FTIR spectra of (a) F127, (b) PU material, and (c) PU-F127 nanospheres.

applied in the evaluation of the *in vitro* antithrombogenicity of biomaterials.[35] The APTT, PT and TT values of saline control for healthy blood plasma were 17.1 ± 0.1, 10.8 ± 0.2 and 13.2 ± 0.1 s, respectively. The effect of PU-F127 nanospheres can be observed by comparing the APTT, PT and TT with those of the saline control. The results showed that the times for the PU-F127 nanospheres were 17.7 ± 0.2, 10.8 ± 0.2 and 13.6 ± 0.3, respectively. Based on the previous research, the anti-coagulation properties of the PU-F127 nanospheres can be attributed to the long PEO chains of F127. More importantly, an antibiofouling surface of GCE can be obtained with the help of the anticoagulation properties of the PU-F127 nanospheres that were immobilized onto the surface of the GCE.

Complement activation and platelet activation

It is known to all that complement activation is a very important parameter of hemocompatibility.[23,24] When a foreign material comes in contact with blood, the complement pathway of the host defense system activates and a series of chemical reactions involving several peptides and enzymes take place, leading to inflammation.[36] In this study, the effect of the PU-F127 nanospheres on complement activation was discussed by incubating the PU-F127 nanospheres with citrate anticoagulated plasma at 37 °C for 1 h. The amount of C3a produced was measured (2.79 ng mL^{-1}), which is neutral and cannot activate the complement system of the whole blood.

Platelet activation upon interaction with samples is another key indicator of blood incompatibility and can lead to thrombotic complications under *in vivo* conditions.[36] The platelet activation was measured after incubating the PU-F127 nanospheres in PRP for 30 min at 37 °C using flow cytometry. Platelet activation is expressed as the percentage of platelets positive for both of the bound antibodies (CD 62P and CD42). PU-F127 nanospheres were found to be neutral to platelet activation and the values (0.43% ± 0.05) were similar to that of the saline control (0.37% ± 0.02). These results are consistent with the previous research work that Pluronic F127 may reduce the inflammatory potential of an external additive.[37–39]

Evaluation of whole blood adhesion tests

The antibiofouling properties of F127 were proved by the previous research work.[12,13] The anti-biofouling properties of the PU-F127 nanospheres were evaluated by whole blood adhesion tests. After being in contact with whole blood for 1 h, the surface morphologies of the blank GCE and GOx–(PU-F127) bioconjugates surfaces were shown in Fig. 3. Numerous adherent blood cells and some aggregates were observed on the blank GCE (Fig. 3a), while blood cells and fibrin adhesion were suppressed substantially on the GOx–(PU-F127) bioconjugates'

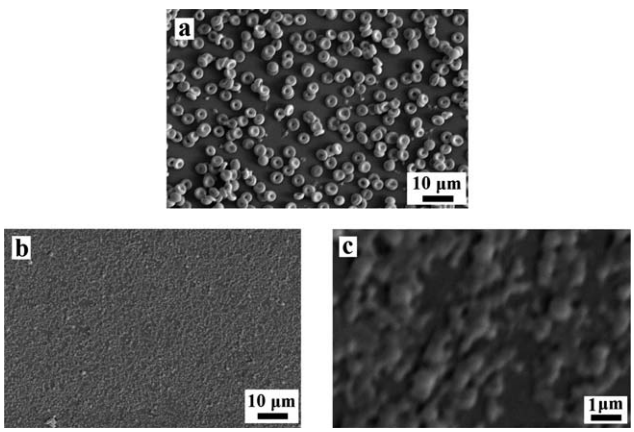

Fig. 3 SEM images of (a) blank electrode substrate, (b) electrode substrate modified with GOx–(PU-F127), and (c) enlarged view from (b) exposed to human whole blood for 60 min.

surfaces (Fig. 3b and c). These results, in conjunction with previous work, suggest that the PU-F127 nanospheres, owing to the hydrated F127 chains attached on the surface, probably influence the microthermodynamics at the whole blood solution–surface interface and prevented adhesion of blood cells.[12] Based on the above observations, it was believed that thrombus was difficult to form on the PU-F127 modified GCE without fused platelets and blood cells. Thus, the PU-F127 nanospheres exhibited a high degree of compatibility and excellent anti-biofouling properties to be applied in whole blood.

Characterization of GOx–(PU-F127) bioconjugates

The retention of enzyme activity on the supporting materials is crucial in biosensor designs, because the secondary conformational variations of the enzyme can affect its activity markedly. Herein, FTIR and CD were utilized to check the secondary conformation variations of the polypeptide chain of GOx on the PU-F127 nanospheres.

As shown in Fig. 4a, two infrared bands of GOx with their center positions at 1644 cm^{-1} and 1541 cm^{-1} can be observed. The former band is related to C═O stretching vibrations of the peptide linkages in the backbone (amide I) and the latter one is ascribed to the combination of C–N stretching and N–H in-plane bending (amide II).[40–42] The demonstration of amide I (1648 cm^{-1}) and amide II (1537 cm^{-1}) in Fig. 4b of the GOx–(PU-F127) bioconjugates indicated that GOx had been adsorbed on the PU-F127 nanospheres. The small shifts of amide I (1644 to 1648 cm^{-1}) and amide II (1541 to 1537 cm^{-1}) of GOx after it was adsorbed on the PU-F127 nanospheres showed that the GOx at the PU-F127 nanospheres' surface did not undergo conformational changes during the process of its immobilization, and remained in its original secondary structure.[43]

CD is one of the most sensitive physical techniques for determining structures and monitoring structural changes of biomolecules. It can directly interpret the changes in protein secondary structure.[44] In the far-UV region (185–260 nm), the spectrum which corresponds to the peptide $n \rightarrow \pi^*$ electronic transitions is sensitive to the changes of the conformation in the active site of GOx.[45] In this present work, CD spectra were used to characterize the secondary structure of GOx before and after bioconjugating with the PU-F127 nanospheres. Fig. 4c showed the CD spectra of GOx and GOx–(PU-F127) bioconjugates. It can be seen that the CD spectrum of the GOx–(PU-F127) bioconjugates was characterized by two negative bands at around 208 and 219 nm (curve i), which looks similar to pure GOx (curve ii) in both peak intensity and peak position. In addition, the contents of α-helix and β-turn conformations of GOx–(PU-F127) changed by 0.1% and 0.1% compared with pure GOx. It is indicated that GOx have been adsorbed on the surface of the nanoparticles, and there is no significant change in the secondary structure of the enzyme in the presence of the PU-F127 nanospheres.[46] These results suggest that the PU-F127 nanospheres indeed have good biocompatibility. Thus, the GOx immobilized on the PU-F127 nanospheres can retain the secondary structure and biological activity in the following electrochemical experiments.

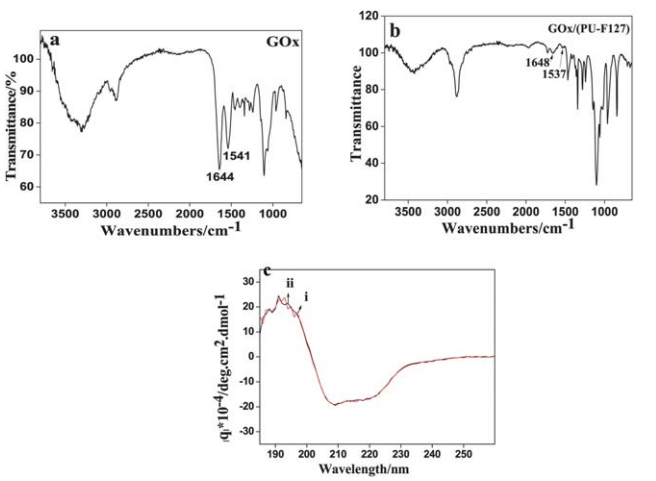

Fig. 4 Characterization of GOx–(PU-F127) bioconjugates. (a) FTIR spectrum of GOx, (b) FTIR spectrum of GOx–(PU-F127) bioconjugates, and (c) CD spectra of (i) GOx–(PU-F127) and (ii) pure GOx in 0.1 M PBS (pH = 7.4) in the wavelength region of 185–260 nm.

Optimization of the glucose biosensor

Various experimental parameters, such as pH value, scan rate, GOx and PU-F127 nanosphere concentrations, may affect the performance of a biosensor. In this work, these parameters were studied to ascertain the optimal working conditions of the glucose biosensor. The relationships between the response current of the fabricated biosensor and various experimental parameters were shown in Fig. 5.

The pH effect on the biosensor performance was investigated by measuring the current response in PBS. A pH value ranging from 5.0 to 9.0 was adopted in this study. As seen in Fig. 5a, compared to the data of response current obtained within other pH value regions, a larger response current was obtained within the range of pH 7.0 to 7.4. However, the normal pH values for arterial whole blood are 7.35 to 7.454; for venous whole blood, 7.36 to 7.41.[47] Thus, the buffer solution was adjusted to pH 7.4 and used in all experiments below.

Fig. 5b shows the effect of scan rate on the response current of the biosensor. The current increased with increasing scan rate until 100 mV s^{-1} and then decreased. Therefore, 100 mV s^{-1} was chosen as the optimal scan rate.

During the biosensor fabrication procedure, the concentration of GOx in PBS may affect the loading amount of the enzyme. Therefore, the effect of the loading amount of GOx on the performance of the biosensor was investigated. The biosensors were constructed with various concentrations of GOx, respectively, and the responses of the prepared biosensors were recorded. The results were presented in Fig. 5c. Increasing the enzyme loading leads to an enhancement in the response current and the response reaches a maximum at a concentration of 6 mg mL^{-1} of GOx. The response of the biosensor decreased at higher concentrations of GOx (for example, 7.5 and 9 mg mL^{-1}). This decrease may be due to the blockage created by the GOx overloading of the PU-F127 nanospheres. Therefore,

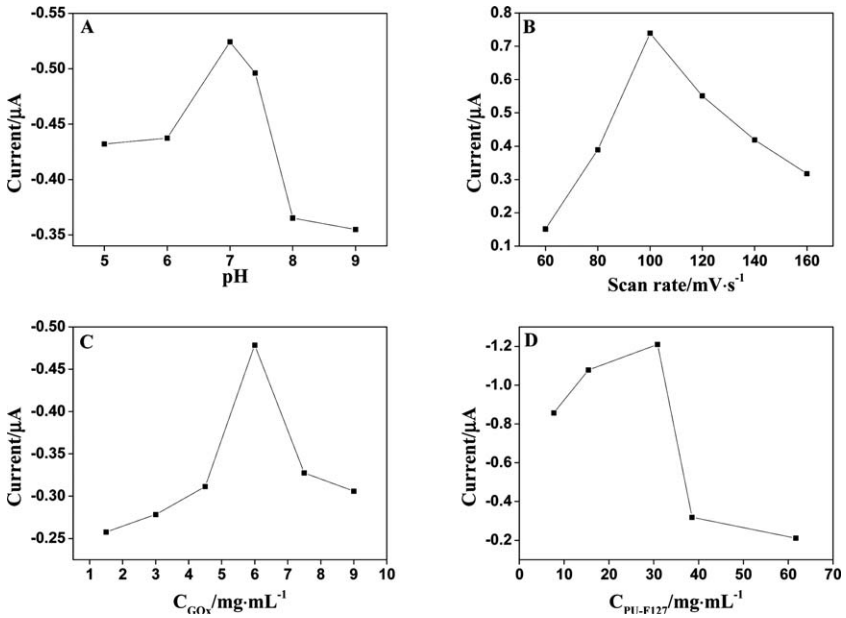

Fig. 5 The amperometric currents of the biosensor varies with (a) the pH value, (b) scan rate, (c) GOx concentration, and (d) PU-F127 concentration.

the electron relaying capacity of the nanospheres may also be disturbed because of the presence of a large amount of insulating and bulky enzyme molecules. Therefore, a concentration of 6 mg mL^{-1} of GOx was chosen as the optimal concentration for construction of the biosensor.

Similarly, a large dependence of response of the biosensor on the PU-F127 nanosphere concentration immobilized was observed, as shown in Fig. 5d. The experimental results showed that the appropriate concentration (30 mg mL^{-1}) was chosen according to the requirements for current response based on the combined effects of enzyme loading efficiency and the electron relaying capacity of PU-F127. In subsequent experiments, 30 mg mL^{-1} PU-F127 nanospheres and 6 mg mL^{-1} GOx solution were compromisingly chosen as suitable concentrations for construction of the biosensor.

Direct electrochemistry of GOx–(PU-F127)–GCE

The CVs of (PU-F127)–GCE, GOx–F127–GCE and GOx–(PU-F127)–GCE in PBS (0.1 M, pH 7.4) were depicted in Fig. 6. No redox peak was observed for the PU-F127 electrode (curve a), suggesting that the PU-F127 nanospheres cannot undergo redox reaction in this potential range. Meanwhile, GOx–F127–GCE (curve b) gave a weak voltammetric signal in the range of −1.0 to 0.2 V. However, the GOx–(PU-F127)–GCE (curve c) showed a pair of well defined and nearly symmetrical redox peaks with the anodic and cathodic peak potentials at −436 and −490 mV (at 100 mV s^{-1}), respectively. Therefore, the pair of peaks in curve c can be ascribed to the direct electron transfer reaction (the conversion of FAD/$FADH_2$ center) of GOx. The separation of the peak potentials (ΔE_p) was 54 mV, indicating that GOx fixed with PU-F127 nanospheres can display a quasi-reversible electrochemical reaction despite its large molecular structure. The results indicated that the bioactivity of GOx was retained because of the mild environment provided by the PU-F127 nanospheres.

Response behavior of the glucose biosensor

Under the optimized conditions, the steady-state amperometric response of the glucose biosensor was investigated by successively adding various concentrations of glucose into 0.1 M PBS (pH 7.4). As shown in Fig. 7, the biosensor has a fast and sensitive response to glucose, and it reaches 95% of the maximum steady state current in 4 s. The inset of Fig. 7 illustrates the calibration plot of response current to different glucose concentrations. A linear response range is obtained from 0.1 mM to 20 mM and the linear regression equation is I (μA) = 0.387c (mM) + 10.13 (R = 0.9994), where I is current and c is the glucose concentration. The apparent surface of the electrode is estimated to be about 0.078 cm^2, and the sensitivity was calculated to be 4.96 μA mM^{-1} cm^{-2}. Additionally, the

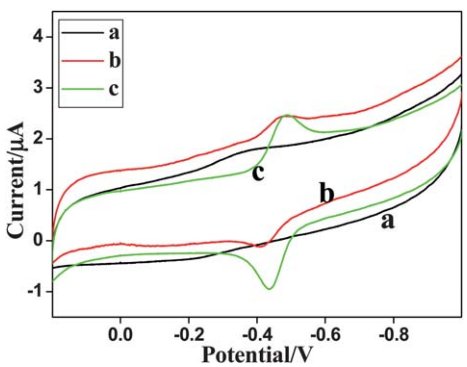

Fig. 6 CV of (a) (PU-F127)–GCE, (b) GOx–F127–GCE, and (c) GOx–(PU-F127)–GCE in 0.1 M PBS (pH = 7.4). Scan rate: 100 mV s^{-1}.

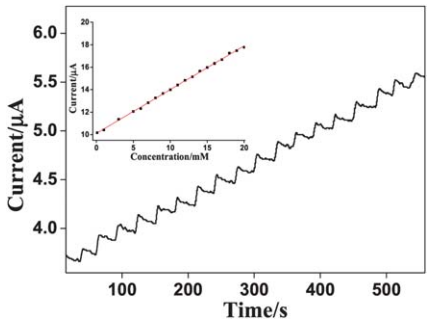

Fig. 7 Amperometric response of the GOx–(PU-F127)–GCE biosensor to successive addition of glucose in PBS (0.1 M, pH 7.4) at an applied potential of −0.49 V, and the inset: calibration curve for glucose obtained at the GOx–(PU-F127)–GCE biosensor.

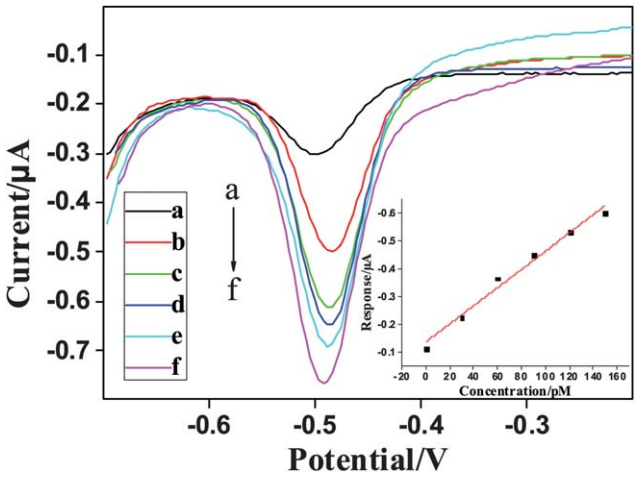

Fig. 8 DPV obtained at GOx–(PU-F127)–GCE in whole blood samples at 25 °C with glucose of (a) 0 pM, (b) 30 pM, (c) 60 pM, (d) 90 pM, (e) 120 pM, (f) 150 pM; and the inset: relationship between the peak current and the concentration of glucose in whole blood samples.

experimental limit of detection (LOD) of the biosensor is measured to be 2.39×10^{-6} M based on a signal–noise ratio of 3 (inset of Fig. 7).

Moreover, an analytical performance comparison of some glucose biosensors reported by previous papers and the novel biosensor we prepared was performed. From Table 1, we can conclude that the proposed biosensor has a higher sensitivity and a lower detection limit than those previous reported models.[48–51] The good performance implies that the PU-F127 nanospheres can provide a good biocompatible microenvironment for maintaining enzymatic activity.

Amperometric determination in whole blood

Fig. 8 showed DPV curves of the GOx–(PU-F127)–GCE biosensor for the successive addition of glucose in whole blood. Blood samples were supplied by a volunteer, within sodium fluoride to prevent glucose metabolism by blood cells prior to glucose determination.[52,53] To mix the added glucose, moderate stirring was carried out for more than 5 min. The DPV curves in Fig. 8 showed that the peak current gradually increased with increasing concentration of glucose and an anodic peak was observed at −0.49 V. The calibration curve by plotting the current response with glucose concentration is presented in the inset of Fig. 8. The linear relation had a regression equation of I (μA) = −0.0033c (pM) − 0.1378 with a correlation coefficient (R) of 0.9911. A detection limit ($S/N = 3$) as low as 1.14×10^{-5} M is observed. These results were due to the biomimetic surface of the PU-F127 nanospheres and the favorable electrical conductivity of the biosensor in whole blood.

Anti-interference and stability studies

Two common interferences existing in biological fluids, namely ascorbic acid (AA) and uric acid (UA) were investigated.[54] When the concentration of glucose was 0.1 mM, the interference effects were investigated by testing the response of the enzyme electrode to 100 times AA and UA. It was found that the substances did not cause any observable interference in the determination of glucose in the presence of AA and UA (Fig. 9a). Thus, the biosensor based on GOx–(PU-F127) has good anti-interference ability.

The reproducibility of the biosensor was also examined by measuring the response in 0.1 M PBS (pH = 7.4). Five biosensors constructed independently give a relative standard deviation (R.S.D.) of 5.6%. As for one biosensor, the R.S.D. is 3.8% for 10 continuous assays. The long-term stability of the biosensor was evaluated by measuring its performance every few days. It can be seen from Fig. 9b that the biosensor retains most of the initial response after 9 days, indicating that the immobilized GOx can efficiently retain their bioactivity for a long time due to the good microenvironment that is provided by the PU-F127 nanospheres.

Table 1 Comparison of analytical performance of some glucose biosensors

Glucose biosensor	Sensitivity (μA mM^{-1} cm^{-2})	Detection limit (M)	Linearity (mM)	Response time (s)	Ref.
Nafion–GOx–OMC	0.053	1.57×10^{-4}	N/A[a]	9	48
GOx–(Au–CH)–Pt	0.555	7×10^{-6}	0.5–16	8	49
GOx–Ferri–CH–SPCE	0.677	1.38×10^{-3}	N/A[a]	20	50
GOx–Fe_3O_4@SiO_2	N/A[a]	3.25×10^{-6}	$(1–4) \times 10^{-5}$	10	51
GOx–(PU-F127)	4.96	2.39×10^{-6}	0.1–20	4	This work

[a] N/A represents relevant data which were not provided in these references.

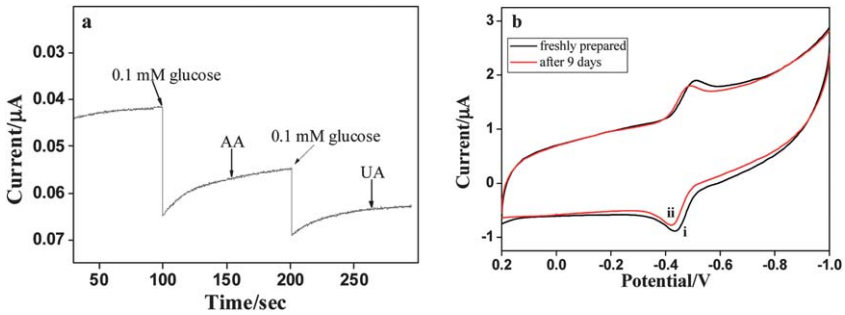

Fig. 9 (a) Amperometric responses of the biosensor upon addition of glucose (0.1 mM), AA (10 mM), glucose (0.1 mM) and UA (10 mM), in PBS. The biosensor was biased on the potential of −0.49 V. (b) CVs of GOx–(PU-F127)–GCE. (i) Freshly prepared, and (ii) after 9 days stored in 0.1 M PBS (pH 7.4). Scan rate was 100 mV s^{-1}.

Real sample analysis

A series of samples were tested in order to demonstrate the practical usage of the biosensor. The results were summarized in Table 2. As can be seen, the values measured by the GOx–(PU-F127)–GCE in our laboratory and hospital biochemistry laboratory are very close. Furthermore, compared to the values measured in serum samples, which are isolated from whole blood, by a biochemical analyzer, the values we measured in whole blood directly by the GOx–(PU-F127)–GCE biosensor are probably more close to the real values. More deeper investigation will be performed by our group.

Conclusion

Nanomaterials with attractive electronic, optical, magnetic, thermal and catalytic properties have attracted great attention due to their widespread applications in physics, chemistry, biology, medicine, materials science and interdisciplinary fields.[55] In this case, the novel PU-F127 nanospheres with anti-biofouling properties were used to construct a special glucose biosensor that can be applied in whole blood directly. The preparation of PU-F127 nanospheres, the GOx–(PU-F127)–GCE biosensor and its electrochemical behavior in whole blood were investigated. The cyclic voltammetric results indicated that GOx immobilized on the PU-F127 nanospheres exhibited direct electron transfer reaction, and the CV displayed a pair of well-defined and nearly symmetric redox peaks with a formal potential of −463 mV. The biosensor had good electrocatalytic activity toward glucose with a low detection limit of 1.14×10^{-5} M in whole blood. The glucose biosensor did not respond to AA and UA at their concentration normally encountered in blood. This idea and method we proposed here provide a promising platform for the development of novel electrochemical biosensors that can be directly used in whole blood systems for component detection of illness diagnosis, and bring new momentum to electrical analysis.

Table 2 Determination of glucose in whole blood samples using GOx–(PU-F127)–GCE

No.	Referenced values[a] (mM)	Determined values[b] (mM)
1	4.1 ± 0.18	3.9 ± 0.16
2	5.3 ± 0.14	5.1 ± 0.23
3	5.7 ± 0.22	5.6 ± 0.21
4	9.8 ± 0.23	9.6 ± 0.25
5	17.6 ± 0.24	17.3 ± 0.28

[a] Referenced values were provided by the hospital biochemistry laboratory. [b] The values were determined by the GOx–(PU-F127)–GCE; they were average values of five measurements for each sample.

Acknowledgements

The work is supported by NSFC (21144002), NSFJS (BK2011781), Major Program for the Natural Science Fundamental Research of the Higher Education Institutions of Jiangsu Province (12KJA150006), the Priority Academic Program Development of Jiangsu Higher Education Institutions, and Base of Production, Education & Research of Prospective Joint Research Project of Jiangsu Province (BY2011109).

References

1 L. D. Chambers, K. R. Stokes, F. C. Walsh and R. J. K. Wood, *Surf. Coat. Technol.*, 2006, **201**, 3642–3652.
2 J. Genzer and K. Efimenko, *Biofouling*, 2006, **22**, 339–360.
3 D. M. Yebra, S. Kiil and K. Dam-Johansen, *Prog. Org. Coat.*, 2004, **50**, 75–104.
4 C. Werner, M. F. Maitz and C. Sperling, *J. Mater. Chem.*, 2007, **17**, 3376–3384.
5 N. Wisniewski and M. Reichert, *Colloids Surf., B*, 2000, **18**, 197–219.
6 V. P. Torchilin, *AAPS J.*, 2007, **9**, 128–147.
7 H. Otsuka, Y. Nagasaki and K. Kataoka, *Adv. Drug Delivery Rev.*, 2003, **55**, 403–419.
8 J. M. Harris and R. B. Chess, *Nat. Rev. Drug Discovery*, 2003, **2**, 214–221.
9 A. Kulkarni, M. Saxena, G. Price, M. J. O'Leary, T. Jacques and J. A. Myburgh, *Intensive Care Med.*, 2005, **31**, 142–145.
10 C. Voulgari and N. Tentolouris, *Diabetes Technol. Ther.*, 2010, **12**, 529–535.
11 M. H. A. Lin, M. C. Wu and J. Lin, *J. Clin. Biochem. Nutr.*, 2010, **47**, 45–52.
12 C. Mao, C. X. Liang, Y. Q. Mao, L. Li, X. M. Hou and J. Shen, *Colloids Surf., B*, 2009, **74**, 362–365.

13 J. H. Lee, Y. M. Ju and D. M. Kim, *Biomaterials*, 2000, **21**, 683–691.
14 M. S. Bakshi, A. Kaura, P. Bhandari, G. Kaur, K. Torigoe and K. Esumi, *J. Nanosci. Nanotechnol.*, 2006, **6**, 1405–1410.
15 C. Mao, X. B. Chen, X. M. Hou, J. Shen, J. J. Zhu and W. B. Zhao, *Gold Bull.*, 2009, **42**, 215–218.
16 A. S. Rad, A. Mirabi, E. Binaian and H. Tayebi, *Int. J. Electrochem. Sci.*, 2011, **6**, 3671–3683.
17 P. R. Solanki, A. Kaushik, V. V. Agrawal and B. D. Malhotra, *NPG Asia Mater.*, 2011, **3**, 17–24.
18 A. Kaushik, R. Khan, P. R. Solanki, P. Pandey, J. Alam, S. Ahmad and B. D. Malhotra, *Biosens. Bioelectron.*, 2008, **24**, 676–683.
19 P. Pandey, M. Datta and B. D. Malhotra, *Anal. Lett.*, 2008, **41**, 159–209.
20 C. Mao, L. C. Jiang, W. P. Luo, H. K. Liu, J. C. Bao, X. H. Huang and J. Shen, *Macromolecules*, 2009, **42**, 9366–9368.
21 H. Murakami, M. Kobayashi, H. Takeuchi and Y. Kawashima, *Int. J. Pharm.*, 1999, **187**, 143–152.
22 L. Wu, Z. Guo, S. Meng, W. Zhong, Q. Du and L. L. Chou, *ACS Appl. Mater. Interfaces*, 2010, **2**, 2781–2788.
23 R. K. Kainthan, M. Gnanamani, M. Ganguli, T. Ghosh, D. E. Brooks, S. Maiti and J. N. Kizhakkedathu, *Biomaterials*, 2006, **27**, 5377–5390.
24 R. K. Kainthan, S. R. Hester, E. Levin, D. V. Devine and D. E. Brooks, *Biomaterials*, 2007, **28**, 4581–4590.
25 S. Alibeik, H. Sheardown, A. S. Rizkalla and K. Mequanint, *J. Biomater. Sci., Polym. Ed.*, 2007, **18**, 1195–1210.
26 C. Mao, C. Liang, W. Luo, J. Bao, J. Shen, X. Hou and W. Zhao, *J. Mater. Chem.*, 2009, **19**, 9025–9029.
27 H. Hu, X. B. Wang, S. L. Xu, W. T. Yang, F. J. Xu, J. Shen and C. Mao, *J. Mater. Chem.*, 2012, **22**, 15362–15369.
28 P. Molina, J. Alcántara and C. López-Leonardo, *Tetrahedron*, 1997, **53**, 3281–3286.
29 T. Sakai and P. Alexandridis, *Langmuir*, 2004, **20**, 8426–8430.
30 P. Innocenzi, L. Malfatti, M. Piccinini and A. Marcelli, *J. Phys. Chem. A*, 2010, **114**, 304–308.
31 F. Tiarks, K. Landfester and M. Antonietti, *J. Polym. Sci., Part A: Polym. Chem.*, 2001, **39**, 2520–2524.
32 V. Durrieu, A. Gandini, M. N. Belgacem, A. Blayo, G. Eiselé and J. L. Putaux, *J. Appl. Polym. Sci.*, 2004, **94**, 700–710.
33 T. Noguchi, *Philos. Trans. R. Soc. London, Ser. B*, 2008, **363**, 1189–1195.
34 F. Patolsky, T. Gabriel and I. Willner, *J. Electroanal. Chem.*, 1999, **479**, 69–73.
35 S. E. Skrabalak, J. Chen, L. Au, X. Lu, X. Li and Y. Xia, *Adv. Mater.*, 2007, **19**, 3177–3184.
36 M. B. Gorbet and M. V. Sefton, *Biomaterials*, 2004, **25**, 5681–5703.
37 J. K. Jackson, C. M. K. Springate, W. L. Hunter and H. M. Burt, *Biomaterials*, 2000, **21**, 1483–1491.
38 A. Kidane and K. Park, *J. Biomed. Mater. Res.*, 1999, **48**, 640–647.
39 D. M. Eckmann, Y. Y. Eckmann and N. Tomczyk, *Combustion Generated Fine Carbonaceous Particles: Proceedings of Interdisciplinary Transport Phenomena VII*, KIT Scientific Publishing, Dresden, 2011.
40 S. Zuo, Y. Teng, H. Yuan and M. Lan, *Sens. Actuators, B*, 2008, **133**, 555–560.
41 J. Li, Y. B. Wang, J. D. Qiu, D. C. Sun and X. H. Xia, *Anal. Bioanal. Chem.*, 2005, **383**, 918–922.
42 L. Wang and Z. Yuan, *Sensors*, 2003, **3**, 544–554.
43 Q. G. Xiao, X. Tao and J. F. Chen, *Ind. Eng. Chem. Res.*, 2007, **46**, 459–463.
44 X. Wu, P. Du, P. Wu and C. Cai, *Electrochim. Acta*, 2008, **54**, 738–743.
45 G. Zoldák, A. Zubrik, A. Musatov, M. Stupák and E. Sedlák, *J. Biol. Chem.*, 2004, **279**, 47601–47609.
46 G. Dai, J. Li and L. Jiang, *Colloids Surf., B*, 2002, **24**, 171–176.
47 A. Waugh and A. Grant, *Anatomy and Physiology in Health and Illness*, Churchill Livingstone Elsevier, Dutch, 2007.
48 M. Zhou, L. Shang, B. Li, L. Huang and S. Dong, *Biosens. Bioelectron.*, 2008, **24**, 442–447.
49 B. Y. Wu, S. H. Hou, F. Yin, J. Li, Z. X. Zhao, J. D. Huang and Q. Chen, *Biosens. Bioelectron.*, 2007, **22**, 838–844.
50 S. H. Lee, H. Y. Fang and W. C. Chen, *Sens. Actuators, B*, 2006, **117**, 236–243.
51 J. Qiu, H. Peng and R. Liang, *Electrochem. Commun.*, 2007, **9**, 2734–2738.
52 D. B. Sacks, D. E. Bruns, D. E. Goldstein, N. K. Maclaren, J. M. McDonald and M. Parrott, *Clin. Chem.*, 2002, **48**, 436–472.
53 A. Chan, R. Swaminathan and C. Cockram, *Clin. Chem.*, 1989, **35**, 315–317.
54 H. Tang, J. Chen, S. Yao, L. Nie, G. Deng and Y. Kuang, *Anal. Biochem.*, 2004, **331**, 89–97.
55 H. Li, S. Liu, Z. Dai, J. Bao and X. Yang, *Sensors*, 2009, **9**, 8547–8561.